Nonlinear control of an inverted pendulum

Samuel Balula[1]

[1]*Physics department, Instituto Superior Técnico, University of Lisbon, Portugal*

The Furuta pendulum is a rotational pendulum that is actuated at its basis by a direct current motor with a gear. Two control problems associated to it consist of swinging-up the pendulum, in order to move it from the downwards position up to the upwards one, and then to equilibrate the pendulum in the upwards position. In both cases, optimal control methods are used. Different aspects related to this problem are considered, that include the selection of an appropriate cost and numerical procedure details. Results show that optimal control is a versatile method for designing trajectories in state space.

I. INTRODUCTION

The aim of this thesis is to develop a control strategy for the nonlinear problem of swinging-up and balancing a Furuta pendulum at its upwards, unstable equilibrium position, using optimal control techniques, and to apply it both in simulation and in a real device. Although this can be seen as an academic problem, this device is illustrative of a wide set of dynamic systems with real-life applications.

This work deals with systems that can be modeled by a finite number of coupled first-order differential equations [1] for a set of variables that define the state of a system *i.e.*, a set of variables that, if known at an instant of time, and together with knowledge about future excitations, fully determines the future behaviour of the system.

A particular case are linear systems, for which powerful analytical tools are available, mostly sustained by the superposition principle.

In the case of nonlinear systems significant progress has been made in recent decades, supported by the increasing computational power available as well as by major advances in theoretical knowledge. They are found in a growing number of state-of-the-art applications, and as so, the field is an active area of research.

One of the simplest examples of a nonlinear system is the rotary pendulum, that is commonly used to illustrate emerging ideas in the field of nonlinear control [2].

Examples include aerospace, industrial, and medical applications [1, 3]. To the author's knowledge, the nonlinear problem of swinging-up the pendulum has never been addressed using optimal control. With this technique the control problem is elegantly formulated as the minimization of a convenient cost, subject to restrictions. The cost function reflects the application requirements, and may yield solutions of minimum time, energy or any other quantity [4].

A. state-of-the-art

The literature on inverted pendulums control is rich and comprises different types of problems and pendulum structures, including for example simple and multiple planar pendulums with an actuator in the base joint [5], mounted on top of a moving cart [6, 7], and rotating pendulums with several geometric variations.

One of the most common methods to perform the swing-up of an inverted pendulum is energy control. In this case the energy of the system is controlled instead of controlling directly its position and velocity [2]. At the end of the procedure the system converges to a homoclinic orbit that drives the state to the unstable equilibrium position [5]. Dissipative forces are generally not considered.

Other methods include energy shaping [8, 9], feedback linearization [10, 11], control Lyapunov functions [12], model predictive control (MPC) [13, 14], minimum attention control and non-parametric methods.

Optimal control deals with the problem of a determining the inputs of a dynamic system that optimize (minimize or maximize) a specified performance index [15]. With an appropriate choice of this cost function, trajectories and control laws can be determined that satisfy the design requirements.

The solution of most real-life optimal control problems relies on numeric methods. A wide variety of methods have been proposed (see [15] and the references therein for an extensive survey, and [16] for example applications and issues), which can be divided in two major classes – indirect and direct methods. Both share the need to integrate the equations that model the system, but perform the optimization process in two distinct ways.

Direct methods transform the optimal control problem into a nonlinear programming (NLP) problem. A general NLP solver is then employed to find the optimal control.

Indirect methods, in which this work focus, rely on the calculus of variations, most specifically using Pontryagin's minimum principle. This approach leads to a multiple-point boundary value problem, whose solutions are extremals, a necessary condition for optimality.

Linear control is a well established subject, with several technologies available that can be employed on the design of controllers and analysis of the resultant system. A classical proportional–integral–derivative controller (PID) is generally the simplest solution, and the most commonly used in industrial applications. Pole placement, root-locus and Linear Quadratic Guassian (LQG) controllers are alternatives to this approach.

LQG controllers have been used with a gain scheduling controller. With gain scheduling different controllers are used at different regions of state space, selected by scheduling variables [17].

B. Original Contributions

A complete model of the Furuta pendulum is developed. It incorporates the characteristic of the electric motor. The parameters of the model are identified form experimental data with a modified version of least squares that takes into account known information about the values of the parameters of the system.

A numeric method is developed as a modification of the steepest descent method. This method yields the optimal nonlinear control for the transition between operation points, with improved convergence over the simple forward-backward integration. The method is tested in simulation and experimentally with a real Furuta pendulum, and in simulation with two other devices.

A technique is developed to find convex sets of points in state space in which a controller is able to stabilize a device. This method is applied to the linear controller used in the upwards position of the Furuta pendulum, described by the nonlinear model developed previously.

A custom made printed circuit board and software has been designed to control the Furuta pendulum. In comparison with the previously available hardware at the laboratory it has an overall cost 2 orders of magnitude below, and improved sensing capabilities. This board provides 4 times more precise readings from the measurements taken by the optical encoders, direct measurement of the motor current and angular speeds. It also comprises a standardized interface over a USB port, making it compatible with any modern computer.

II. MODEL

Models are a key component to controller design. In addition, they allow to simulate the system and test control approaches in a preliminary phase. In some cases, such as nonlinear Model based Predictive Control (MPC), the control algorithm requires a plant model to be embedded in the decision taken in real time about the value of the manipulated variable.

A nonlinear model of the Furuta Pendulum is constructed from the geometry of the system using Lagrangian mechanics.

The model obtained is the following

$$
\begin{cases}
\dot{x}_1 = & x_2 \\
\dot{x}_2 = & \Big\{ -J_2\big[K_{a1}x_2 - K_f x_5 + x_4(L_{cm2}L_{e1}m_2 x_4 + 2J_2 x_2 \cos x_3)\sin x_3\big] \\
& + L_{cm2}L_{e1}m_2 \cos x_3\big[-K_{a2}x_4 + (gL_{cm2}m_2 + J_2 x_2^2 \cos x_3)\sin x_3\big]\Big\}\Big/ \\
& \big[-L_{cm2}^2 L_{e1}^2 m_2^2 \cos^2 x_3 + J_2(J_0 + J_2 \sin^2 x_3)\big] \\
\dot{x}_3 = & x_4 \\
\dot{x}_4 = & \Big\{K_{a2}x_4 - gL_{cm2}m_2 \sin(x_3)(J_0 + J_2 \sin^2 x_3) + \\
& \cos x_3\big[(-J_0 J_2 x_2^2 + L_{cm2}^2 L_{e1}^2 m_2^2 x_4^2)\sin x_3 - \\
& J_2^2 x_2^2 \sin^3 x_3 + L_{cm2}L_{e1}m_2(K_{a1}x_2 - K_f x_5 + J_2 x_2 x_4 \sin(2x_3))\big]\Big\}\Big/ \\
& \big[L_{cm2}^2 L_{e1}^2 m_2^2 \cos^2 x_3 - J_2(J_0 + J_2 \sin^2 x_3)\big] \\
\dot{x}_5 = & (-K_t x_2 - R x_5 + u)/L_b
\end{cases}
\tag{1}
$$

where $J_0 = I_{xx1} + L_{cm1}^2 m_1 + L_{e1}^2 m_2$ and $J_2 = I_{xx2} + L_{cm2}^2 m2$, m_1 is the mass of the horizontal arm, L_{cm1} the distance from axis of rotation to centre of mass of the horizontal arm, L_{e1} the lenght of the horizontal arm, K_{a1} the friction coeficient between base and the horizontal arm, I_{xx1} the moment of inertia component at the centre of mass along the x axis of the horizontal arm, J_0 the moment of inertia at the base joint of the horizontal arm and pendulum, m_2 the mass of the pendulum, L_{cm2} the distance from axis of rotation to centre of mass of the pendulum, L_{e2} the lenght of the pendulum, K_{a2} the friction coeficient between the horizontal arm and the pendulum, I_{xx2} the moment of inertia component at the centre of mass along the x axis of the pendulum, J_2 the moment of inertia at the joint of the pendulum, L_b te electric impendance of the motor (imaginary part), R the electric internal resistance of the motor, K_t the counter-electromotive force term, coupling the angular speed and current of the motor, and K_f the torque produced by the motor per current unit.

The state variables are the angular position x_1 and velocity x_2 of the horizontal arm, the angular position x_3 and velocity x_4 of the pendulum and the current of the motor x_5.

Tabela I: Identified parameters with least squares method

Parameter	Value	Unit
L_{e1}	227 ± 1	mm
J_0	86.98 ± 0.03	$\mathrm{g \cdot m^2}$
K_{a1}	1.0 ± 0.3	$\mathrm{mN \cdot m \cdot s}$
M_2	309 ± 1	g
L_{cm2}	404 ± 1	mm
J_2	28.37 ± 0.01	$\mathrm{g \cdot m^2}$
K_{a2}	0.136 ± 0.001	$\mathrm{mN \cdot m \cdot s}$
L_b	3.0 ± 0.1	mH
R	2.266 ± 0.002	Ω
K_t	0.696 ± 0.001	$\mathrm{V \cdot s}$
K_f	3.377 ± 0.002	$\mathrm{V \cdot s}$

A. Parameter estimation

Some of the parameters of the model may be readily measured, while others, such as the friction coefficients or inertia moments, might require disassembling the apparatus to enable a precise measurement. Apart from using the manufacturer standard values for physical quantities, experimental data (from the sensors available in the device) enables the estimation of all relevant parameters.

Parameter estimation from experimental data can be performed with a least squares method. However, due to the high number of free parameters in the model and numeric instabilities for certain sets of parameters, it is convenient to take into account the known information provided by the manufacturer.

Assuming that the observations follow a normal distribution, the Bayesian estimate is obtained [18] by minimizing J_N with respect to θ:

$$J_N(\theta) = \sum_{i=1}^{n_\theta} \left(\frac{1}{\sigma_i} (\theta_i - \bar{\theta}_i)^2 \right) + \sum_{j=1}^{n_p} \sum_{k=1}^{n_y} \left(\frac{1}{\sigma_{jk}^2} \left(y_{jk} - \hat{y}_{jk}(\theta) \right)^2 \right), \tag{2}$$

where the first term is a prior, that penalizes deviations of the parameters from the reference value. The weights σ_i measure the confidence on the value of the prior estimate. The second term accounts for the differences between the model output and the experimental data, for a set of n_p points with dimensions n_y. The weights σ_{jk} measures the confidence on the experimental point j of output channel k.

Note that the system is described by a set of differential equations for which there is no known closed form solution. For that reason, the differential equation system must be integrated at each iteration of the least squares with a suitable numerical integration method, that provides the numeric values $\hat{\mathbf{y}}_j(\theta) = C\hat{\mathbf{x}}_j(\theta)$ for the same times t_j as the experimental data $\mathbf{y}_j$ (figure 1).

The results of the identification are presented in table I.

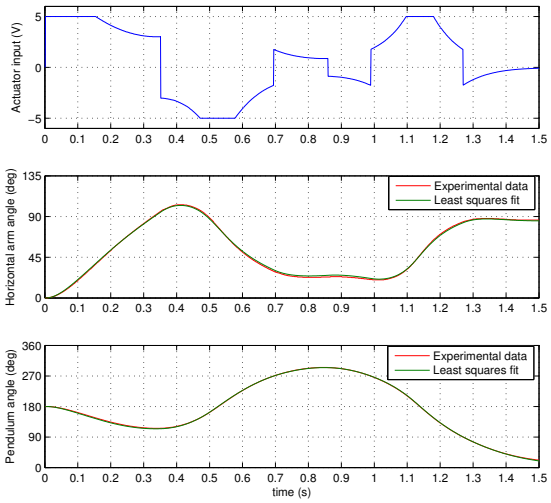

Figura 1: Swing-up of the Furuta pendulum using exponentiation, with $n = 2.15$, $k_v = 0.665$. Model fitted to experimental data using least-squares method with weighting and regularization, parameters presented in table I. $\chi^2_{ndf} = 8.7$. Error bars omitted for readability: all experimental points have 0.35 deg systematic errors.

The non-linear system can be linearised by taking the linear terms of the Taylor series around an operation point, and made discrete for a constant time interval h with

$$\Phi = e^{Ah}, \tag{3a}$$

$$\Gamma = \int_0^h e^{A\tau} d\tau b, \tag{3b}$$

with which the discrete linear model can be written as

$$\begin{cases} x(t_{k+1}) = \Phi x(t_k) + \Gamma u(t_k) \\ y(t_k) = Cx(t_k) + Du(t_k) \\ t_k = t_0 + hk \end{cases} . \tag{4}$$

Eigenvalues were computed for several operation points along with controllability and observability, and asymptotic stability evaluated for the two fixed points of the system (table II A). The last eigenvalue is associated with the eigenvector $(1, 0, 0, 0, 0)$. As it is always zero, the dynamics on the state-variable X_1 are neither stable or unstable. This is due to the fact that the system has cylindrical symmetry.

III. PLANNING

Trajectory planning is the problem of finding the inputs that make a dynamic system execute a desirable trajectory in state-space, *i.e.* a trajectory that complies

X_3	Eigenvalues					A. Stable	Controllable	Observable
	1	2	3	4	5			
0	-737.2	-19.4	$+7.0$	-5.8	0	No	Yes	Yes
$\pi/4$	-743.2	-11.8	-5.3	$+5.0$	0	–	Yes	Yes
$\pi/2$	-746.2	-9.1	-0.0	0	0	–	No	Yes
$3\pi/4$	-743.2	-12.4	$+0.1+5.0i$	$+0.1-5.0i$	0	–	Yes	Yes
π	-737.2	-17.0	$-0.5+6.8i$	$-0.5-6.8i$	0	Yes	Yes	Yes

with the constraints and, if possible, optimizes a specified quantity.

Although several strategies can be used to design trajectories, the focus is given to optimal control. This technique provides a clear framework for finding solutions for problems subject to constraints and optimization goals.

With the Furuta Pendulum as the case study, several strategies have been employed to perform the swing-up, both in simulation and with the real device.

A. Ad hoc methods

In [14] a control law is proposed for the swing-up of the Furuta pendulum, based on energy control, but modified to use only the state variables of the system. The control is given by

$$u = sat\left(k_v \ |\beta^n|\right) \ sign\left(\dot{\beta} \ \cos\beta\right), \tag{5}$$

the first term takes the angle between the current position and vertical. A exponent n is added to the expression, which makes the amplitude of the input greater when the pendulum is far from the upwards position, but smaller when it is closer. The second term defines the sign of the control input, and assures that the input effect is to add energy to the system.

Other ad hoc methods have been used, such as energy shaping and energy control.

B. Optimal control

Let $\mathbf{x}(t)$ be the trajectory in state space of the dynamic system with equations of motion

$$\dot{\mathbf{x}} = f[\mathbf{x}(t), u(t)], \tag{6}$$

with initial conditions

$$\mathbf{x}(t_0) = \mathbf{x}_i \tag{7}$$

and the cost function $J\left[u(t)\right]$ be in the Bolza form

$$J[u(t)] = \Psi\left[\mathbf{x}(T)\right] + \int_{t_0}^{T} \mathcal{L}\left[\mathbf{x}(t), u(t)\right] dt \tag{8}$$

where $\mathbf{x} \in \mathbb{R}^n$ is the state vector, u is the input variable, that takes values in the space of admissible controls $\mathcal{U}$, T is the terminal time, $\Psi\left[\mathbf{x}(T)\right]$ is the cost term on the terminal state, and $\mathcal{L}\left[\mathbf{x}(t), u(t)\right]$ a function that evaluates the cost during the transient, that is designated either as the Lagrangian or the running cost.

The goal of the optimization process is to minimize the cost function while complying with the constraints

$$\begin{cases} \min & J\left[u(t)\right], \\ s.t. & \dot{\mathbf{x}} = f[\mathbf{x}(t), u(t)], \\ & \mathbf{x}(t_0) = \mathbf{x}_i, \\ & u(t) \in \mathcal{U}, \\ & t \in [t_0, T], \end{cases} \tag{9}$$

where the constraints on the terminal state are not set.

Pontryagin's minimum principle gives a necessary condition for the solution of (9). Let $\mathcal{H}$ be the Hamiltonian, defined as

$$\mathcal{H}\left[\boldsymbol{\lambda}(t), \mathbf{x}(t), u(t)\right] = \boldsymbol{\lambda}'(t) \ f\left[\mathbf{x}(t), u(t)\right] + \mathcal{L}\left[\mathbf{x}(t), u(t)\right], \tag{10}$$

where a co-state $\boldsymbol{\lambda}(t) \in \mathbb{R}^n$ is introduced, and the Hamilton equations hold

$$\frac{d\boldsymbol{\lambda}}{dt} = -\frac{\partial \mathcal{H}}{\partial \mathbf{x}}, \tag{11a}$$

$$\frac{d\mathbf{x}}{dt} = +\frac{\partial \mathcal{H}}{\partial \boldsymbol{\lambda}}, \tag{11b}$$

where (11b) is simply (6), and (11a) can be expressed as

$$-\dot{\boldsymbol{\lambda}}' = \boldsymbol{\lambda}' \ f_{\mathbf{x}}\left[\mathbf{x}(t), u(t)\right] + \mathcal{L}_{\mathbf{x}}\left[\mathbf{x}(t), u(t)\right], \tag{12}$$

with the boundary condition

$$\boldsymbol{\lambda}'(T) = \Psi_{\mathbf{x}}\left[\mathbf{x}(T)\right], \tag{13}$$

where the subscript applied to a function represents the partial derivative with respect to the subscript ($\mathcal{F}_{\mathbf{x}} \equiv \nabla_{\mathbf{x}}\mathcal{F}$), and the prime superscript designates the transpose ($\mathcal{M}' \equiv \mathcal{M}^T$). This notation is adopted for simplicity of writing and to avoid confusion with T, the terminal time.

Pontryagin's minimum principle states that the optimal control input $u^*(t)$ minimizes the Hamiltonian $\mathcal{H}$ at every instant $t \in [t_0, T]$. A formal statement of the theorem can be found in [19, p. 94].

Since the input variable is bounded, the minimum can occur in two situations, that have to be evaluated separately

1. at a boundary of $\mathcal{U}$;

2. in the interior of $\mathcal{U}$.

Let the cost function be of the particular form

$$J\left[u(t)\right] = \frac{1}{2}\ \gamma_1\ \mathbf{x}'(T)\ Q_1\ \mathbf{x}(T) + \int_0^T \left(\frac{1}{2}\ \gamma_2\ \mathbf{x}'(t)\ Q_2\ \mathbf{x}(t) + \frac{1}{p}\ \gamma_3\ |u(t)|^p\right) dt, \tag{14}$$

where $\gamma_i \in \mathbb{R}$, and $Q_i \in \mathbb{R}^{n\times n}$ is by convention normalized. Although this form is not general, many problems can be written in this manner. It allows for the description of problems with a quadratic cost on the terminal and transient states, and an arbitrary exponent to the control function. In this case the following equations hold

$$\Psi\left[\mathbf{x}(T)\right] = \frac{1}{2}\ \gamma_1\ \mathbf{x}'(T)\ Q_1\ \mathbf{x}(T) \tag{15}$$

$$\Psi_{\mathbf{x}}\left[\mathbf{x}(T)\right] = \gamma_1\ \mathbf{x}'(T)\ Q_1 \tag{16}$$

$$\mathcal{L}\left[\mathbf{x}(t), u(t)\right] = \frac{1}{2}\ \gamma_2\ \mathbf{x}'(t)\ Q_2\ \mathbf{x}(t) + \frac{1}{p}\ \gamma_3\ |u(t)|^p \tag{17}$$

$$\mathcal{L}_{\mathbf{x}}\left[\mathbf{x}(t), u(t)\right] = \gamma_2\ \mathbf{x}'(t)\ Q_2 \tag{18}$$

The problem is now a set of $2n$ first-order differential equations. There are n equations of motion in a state-space form (6) where the boundary conditions apply at $t = 0$, and n co-state equations (12) where the boundary conditions are set for $t = T$.

While for $p = 2$ and linear dynamics this problem has a well known solution, the LQR, in general a suitable numerical method must be used to solve this problem.

The weights γ_i define the relative importance given to each component of the cost function. If $\gamma_1 \gg \gamma_2, \gamma_3$, the first term is dominant, and therefore the optimal trajectory will mostly optimize the terminal state, eventually with a very costly control input and disregarding the transient states. This situation reduces the stability of the numeric methods. On the contrary, the terms inside the integral improve the stability of the numeric method, and result in smoother solutions. However, the distance to the desired terminal state increases.

C. FP Optimization with L_2 ($p = 2$)

When (14) has $p = 2$, the cost function is said to result from the L_2 norm. The term on u^2 has the physical characteristics of power, and its integral of energy. Taking the model of the FP (1) and using the software *Mathematica* to perform symbolic manipulation, the Hamiltonian can be evaluated from its expression (10). For the computation of the optimal control only the terms dependent on u, $\mathcal{H}(u)$, are of interest. These can be written as

$$\mathcal{H}(u) = \frac{\lambda_5}{L_b}u + \frac{1}{2}\gamma_3 u^2, \tag{19}$$

which is a function in $\mathcal{U} \to \mathbb{R}$. Pontryagin's minimum principles requires $\mathcal{H}(u)$ to be minimum for every time instant for $u*$ to be optimal. If the minimum is in the interior of $\mathcal{U}$, then it can be found with the zero of the first partial derivative with respect to u (it is a minimum due to convexity of the function, as $\gamma_3 > 0$)

$$\frac{\partial \mathcal{H}(u)}{\partial u} = \frac{\lambda_5}{L_b} + \gamma_3 u = 0, \tag{20}$$

which can be rewritten in order to u

$$u^*(t) = -\frac{\lambda_5(t)}{\gamma_3 L_b}, \tag{21}$$

as the input variable is bounded, the minimum of $\mathcal{H}(u)$ can also occur at a boundary of $\mathcal{U}$. In general the value at each boundary must be evaluated to find the minimum. The minimum is found for each time instant $t \in [t_0, T]$, which could be done symbolically for simple problems, but is unfeasible in this case. Hence, the time domain must be made discrete, and the optimization performed for each step (figure 2).

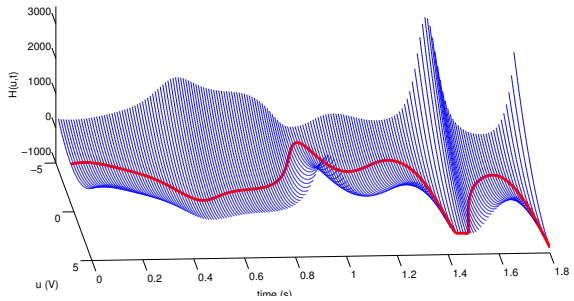

Figura 2: Optimization performed for the FP with L_2 norm, at iteration 1000 of the numerical method. The red line shows the optimal value $u^*(t)$, that corresponds to the minimum of $\mathcal{H}(u, t)$ for every time instant.

D. FP Optimization with L_1 ($p = 1$)

When (14) has $p = 1$ the cost function is said to be of L_1 norm. In this case the Hamiltonian terms dependent on u, $\mathcal{H}(u)$ may be written as

$$\mathcal{H}(u) = \frac{\lambda_5}{L_b}u + \gamma_3\,|u|\,. \tag{22}$$

The analysis of this case is clearer in a graphical way (figure 3). The expression for u^* is

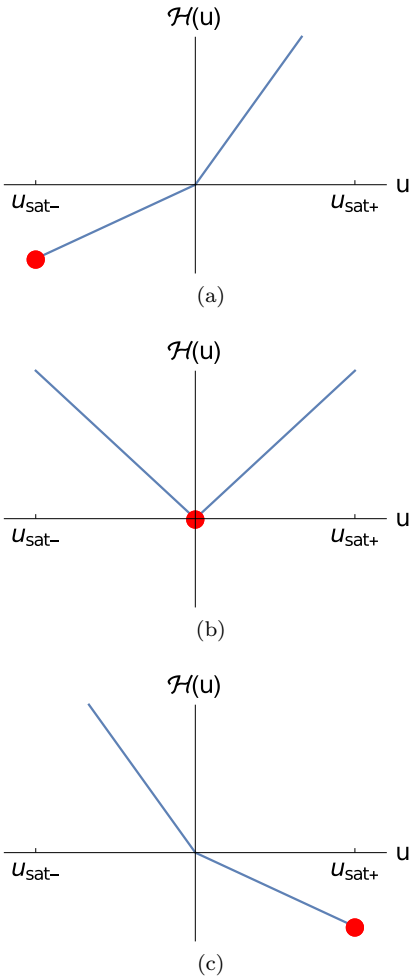

Figura 3: Hamiltonian terms dependent on u with L1 norm for $\gamma_3 L_b < \lambda_5$ (a), $-\gamma_3 L_b < \lambda_5 < \gamma_3 L_b$ (b), $\lambda_5 < -\gamma_3 L_b$ (c). The bold point marks the minimum of the function.

$$u^* = \begin{cases} u_{sat-} \ , & \gamma_3 L_b < \lambda_5 \\ 0 \ , & -\gamma_3 L_b \leq \lambda_5 \leq \gamma_3 L_b \ . \\ u_{sat+} \ , & \lambda_5 < -\gamma_3 L_b \end{cases} \tag{23}$$

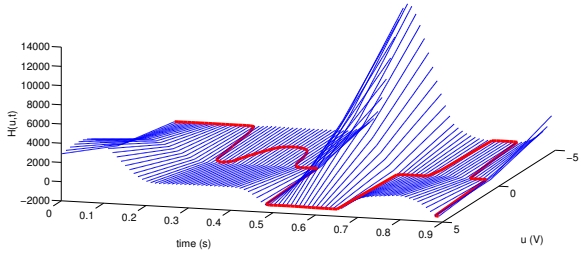

Figura 4: Optimization performed for the FP with L1 norm, at iteration 2000 of the numerical method. The red line shows the optimal value $u^*(t)$, that corresponds to the minimum of $\mathcal{H}(u,t)$ for every time instant.

IV. CONTROL HARDWARE

Two different control system are employed to test and apply the developed model

1. a commercial, off-the-shelf solution acquired from the manufacturer *National Instruments*. It is composed by a personal computer (PC), running *Matlab/Simulink*, a PCI-6040E board (DAQ) connected to the PC at a PCI port, and an analog amplifier. The sensors – optical quadrature encoders (QE) – at the joints of the FP are connected to the DAQ directly. The actuator signal, produced by a digital to analog converter (DAC) at the DAQ is first amplified by the external analog amplifier before being applied to the motor.

2. a custom made board, designed and produced by the author, capable of controlling the device without external components. It incorporates the functions of the DAC, PC, and analog amplifier of the commercial solution, and provides additional functions such as current measurement and analog filtering. The QE are connected to this board directly.

The motivation for the development of the control system derive from a number of shortcomings of the commercial solution, when applied to the FP:

Encoder resolution – the DAQ does not have a native quadrature encoder interface, instead, the up/down counters are used, which reduces the resolution of the sensors by a factor 4. Thus in this configuration the reading of the sensors have 1024 levels per revolution, instead of the 4096 available if adequate hardware was used;

Unmeasured states – only 3 in 5 of the states variables can be measured directly: the angular positions of both links with quadrature encoders and the speed of the horizontal arm with a tachometer. It is not possible to measure directly the speed of the pendulum, since the timers are already being used as counters, or the current of the motor, since the amplifier does not provide sensing capabilities;

Cost – the estimated cost of the control electronics is $>$ 3000 EUR. To this price adds the licenses for the proprietary software compatible with this DAQ;

Deployment time – using *Matlab/Simulink* the time required to compile and deploy the program is about 60 s;

Reliability – as the control software grows in complexity, the development environment is subject to frequent errors which often require the restart of the PC. It is clear that a system with this configuration could not be used in a production environment.

The components of the board were chosen to abbey to the defined requirements, but also to provide versatility, while maintaining costs as low as possible. The circuit has a modular configuration, in which not all components must be soldered, if they are not to be used, or can be

turned off by an appropriate choice of the jumper configuration.

The Printed Circuit Board (PCB) (figure 5) was designed with separate zones and associated ground planes according to their functionality: digital, analog and power. It comprises redundant connections: screw terminals and male headers. The format is a standard 3U Eurocard with 100 mm × 160 mm, and is fabricated in a double layer board. Components are mounted in the top layer, except for the female headers that connect to the RPi, that populates the bottom layer.

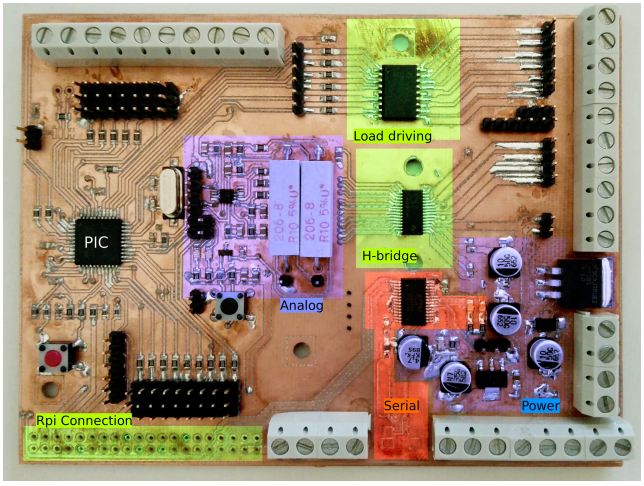

Figura 5: Custom made controller board with essential components soldered. The colours identify each functional zone.

The software implements the algorithm for swing-up using exponentiation of the pendulum position and equilibrium with a LQR controller. Note that a LQG was not implemented since all states are measured directly, although the use of a estimator could improve the performance of the control.

V. RESULTS

The optimal control calculated with L_2 norm in III C was applied to the real device (figure 6). The reference input was corrected by the gain scheduling controller, which accounts for the differences between the reference and the output variables, and actuates on the input to approximate the behaviour of the system to the one predicted in simulation.

In a similar way, the reference produced with the L_1 norm in III D, was applied to the real device (figure 7).

In both cases, after the finish of the swing-up, the reference was set to zero for both input and output variables.

The swing-up was also performed experimentally with energy shaping, and exponentiation of the pendulum position.

The equilibrium was maintained with two different LQG controllers, one continuous (figure 8) and one discrete (figure 9). The equilibrium achieved with the custom made control system (10) has lower variance when compared with the control performed with the commercial solution. However, the angle of the horizontal arm has a oscillatory characteristic with a period of about 8s.

Figure 11 show that the area in which the linear con-

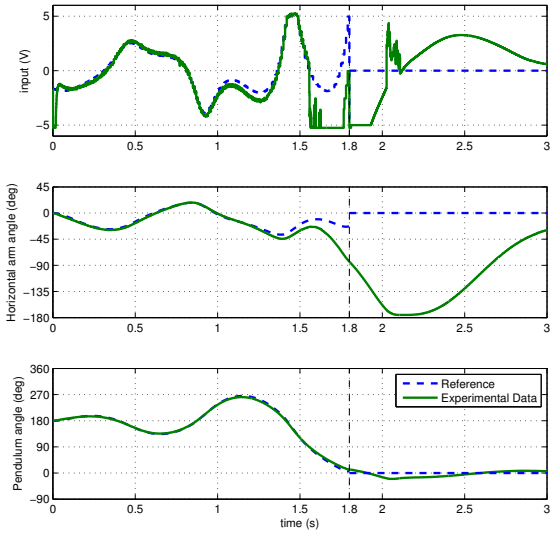

Figura 6: Swing-up performed with optimal control (L_2 norm). Input applied from reference and corrected with a gain scheduling controller. After $t = 1.8s$ the references for the input and output are set to zero. Sampling time 1ms.

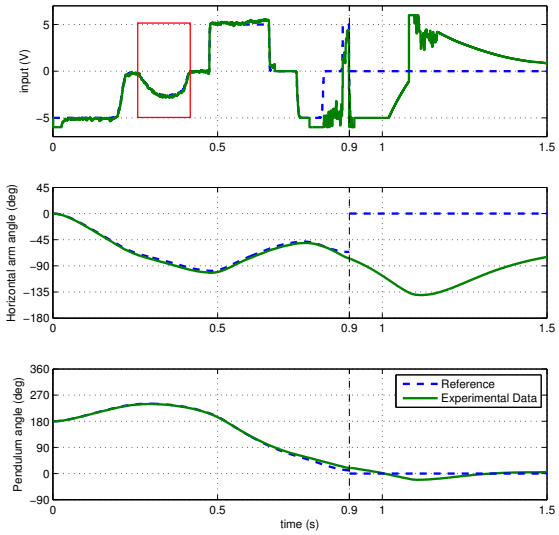

Figura 7: Swing-up performed with optimal control (L_1 norm). Input applied from reference and corrected with a gain scheduling controller. After $t = 0.9s$ the references for the input and output are set to zero. Sampling time 1ms.

troller is able to stabilize the non linear system increase as a function of the maximum input amplitude defined.

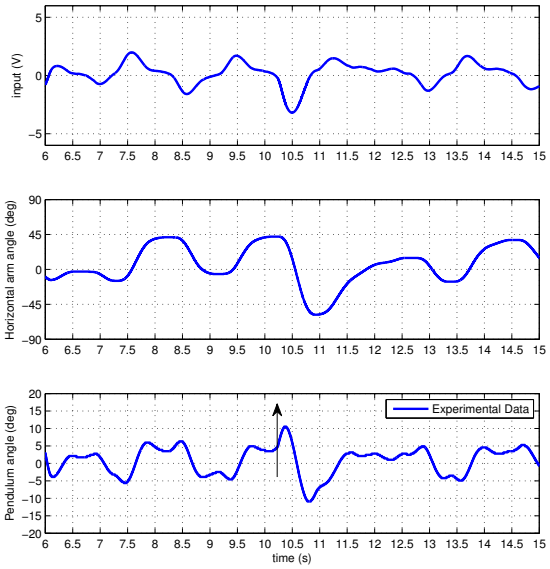

Figura 8: Equilibrium maintained with a continuous LQG controller. The arrow indicates an external perturbation applied to the pendulum. Sampling time 1ms.

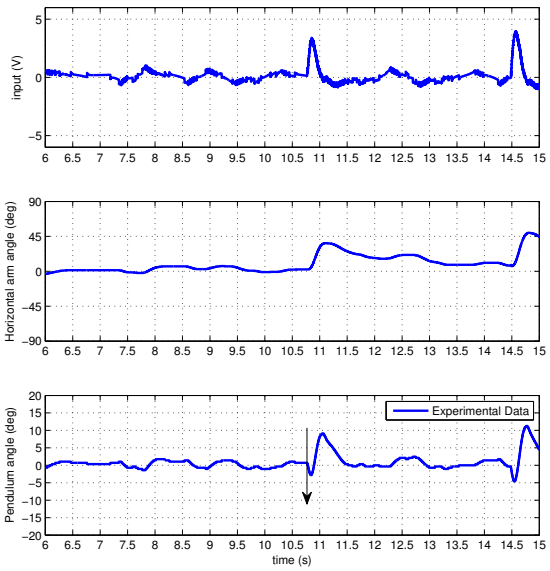

Figura 9: Equilibrium maintained with a discrete LQG controller. The arrow indicates an external perturbation applied to the pendulum. Sampling time 1ms.

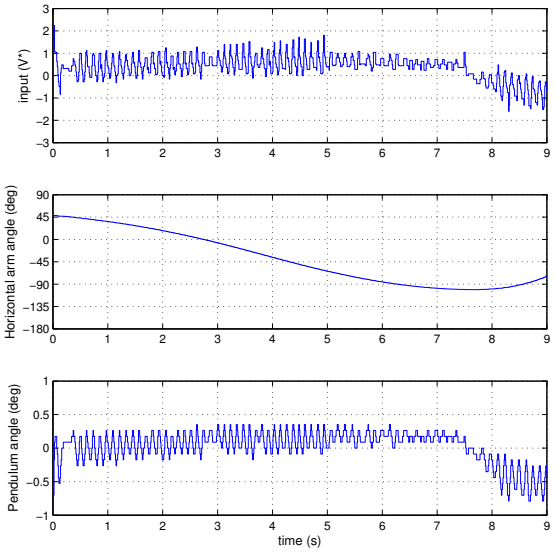

Figura 10: Equilibrium maintained with a discrete LQR controller immediately after swing-up, using the custom made control system. Sampling time 10ms, control period 250μs. This data set does not contain external perturbations, besides the initial offset due to the end of the swing-up manoeuvre, which has been omitted due to the different y-magnitudes involved.

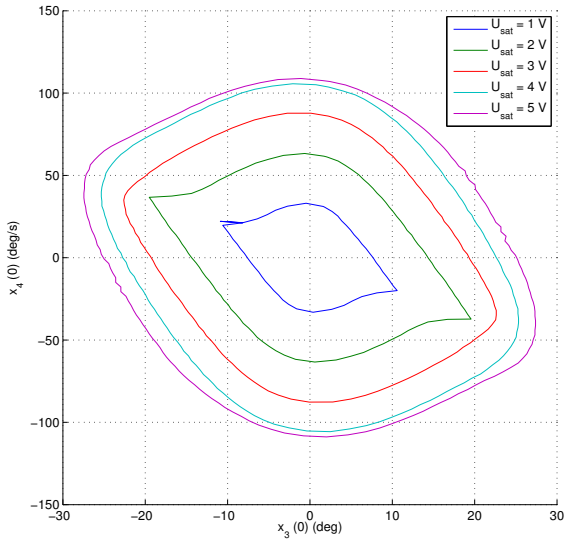

Figura 11: FP initial conditions in which equilibrium is achieved, as a function of the allowed amplitude for u, where the lines represent the boundary of the region of attraction. $x_1(0)$, $x_2(0)$ and $x_5(0)$ are set to zero. Simulations are performed with the non linear model using *Matlab/Simulink* and the continuous LQG controller.

VI. CONCLUSION

Results show that optimal control is an effective method to calculate state space trajectories for the FP, an under-actuated system with non linear dynamics. The characteristics of the control function and trajectory generated can be altered by an appropriate choice of the cost function structure and weights. Results also suggest that the method can be applied to a wide range of system with different characteristics, if an appropriate numerical method is used.

Results also show that the gain scheduling controller is an effective way to have a nonlinear system follow a reference trajectory. Transitions between controllers can be made smooth, although this requires a trade-off with the speed of reaction.

Contrary to one could expect, when designing an equilibrium controller, it is more difficult to maintain the angle of the horizontal arm within bounds than the pendulum at its upwards position.

A. Achievements

A complete model of the system is developed, which captures the dynamics of the FP and actuator. The simulations performed with this model are in agreement with experimental data. The accuracy of the model allows for the design of controllers in a simulated environment, and a hassle-free transition to the real device. Both a global nonlinear and local linear models (continuous and discrete) are produced.

The numerical method for optimal control proposed in this work found solutions not only for the problem of swinging-up the FP, but for other unrelated systems such a wave energy converter. It offers improved stability over other methods such as FBS which failed to converge in both cases.

A technique is proposed and used to find the regions of attraction of a controller, but can also be used in any dynamic system as long as it fulfils the sufficient condition of this region being convex.

Equilibrium is achieved reliably with the use of both a continuous and discrete LQG controllers. They are able to stabilize the plant in the event of external perturbations. They are shown to be limited in their region of attraction by the power of the actuator.The method used to evaluate this region is original and general.

A custom made control system is developed and tested. Results show improved reliability when compared with the previously available commercial solution, which is 2 orders of magnitudes costlier. The new system is more compact and flexible, providing sensing capabilities for all 5 state space variables. The equilibrium achieved with this system has improved variance over the obtained with the commercial solution. This board may be used in the future to control a wide range of devices without additional external components, for example in a classroom environment.

B. Future Work

During the development of this work, several divergent lines of research or possible analysis were identified. However, given the time limitations for this thesis development, they have not been addressed:

Other techniques can be used to model the system, which can be specially useful when there is no information available about its structure, for example neural networks;

There is a wide number of numerical methods available that allow the calculation of optimal trajectories (and respective control inputs). Since the FP and related simplified systems proved to be a useful test ground, it is of interest to compare the performance of each of this methods systematically, using the results of simulations and experiments with the real device. This comparison could be done for several aspects, for example the cost as a function of the computational power required, or the robustness of the method, and could be done for gradient, shooting, and pseudo-spectral methods for example;

With an appropriate cost function it should be possible to find minimum time trajectories, which are of interest in many applications;

The terminal state may be imposed, instead of contributing to the cost function;

Optimal control can be performed in discrete time, it would be of interest to analyse the differences to the continuous case;

The numerical method proposed in this work could be applied to different systems, specially to ones where other methods have difficulties;

A systematic study of the effects of having sensors for all states in the performance of the controller would be of interest.

Finally, a study of the limits of performance of positioning, when equilibrating the pendulum.

[1] Hassan K Khalil and JW Grizzle. *Nonlinear systems*, volume 3. Prentice hall New Jersey, 1996.

[2] Karl Johan Åström and Katsuhisa Furuta. Swinging up a pendulum by energy control. *Automatica*, 36(2):287–295, 2000.

[3] Jean-Jacques E Slotine, Weiping Li, et al. *Applied nonlinear control*, volume 199. prentice-Hall Englewood Cliffs, NJ, 1991.

[4] Arthur Earl Bryson and Yu-Chi Ho. *Applied optimal control: optimization, estimation and control*. CRC Press,

1975.

[5] Isabelle Fantoni, Rogelio Lozano, Mark W Spong, et al. Energy based control of the pendubot. *IEEE Transactions on Automatic Control*, 45(4):725–729, 2000.

[6] Qifeng Wei, Wijesuriya P Dayawansa, and WS Levine. Nonlinear controller for an inverted pendulum having restricted travel. *Automatica*, 31(6):841–850, 1995.

[7] Jesús Patricio Ordaz Oliver and Virgilio López Morales. Control based on swing up and balancing scheme for an experimental underactuated robot. In *Electronics, Robotics and Automotive Mechanics Conference, 2007. CERMA 2007*, pages 512–517. IEEE, 2007.

[8] Romeo Ortega, Arjan J. van der Schaft, Iven Mareels, and Bernhard Maschke. *Energy shaping control revisited*, pages 277–307. Springer London, London, 2001.

[9] Sujit Nair and Naomi Ehrich Leonard. A normal form for energy shaping: application to the furuta pendulum. In *Decision and Control, 2002, Proceedings of the 41st IEEE Conference on*, volume 1, pages 516–521. IEEE, 2002.

[10] Kevin Groves and Andrea Serrani. Modeling and nonlinear control of a single-link flexible joint manipulator. *APPENDICES*, 2004.

[11] K Guemghar, B Srinivasan, Ph Mullhaupt, and D Bonvin. Analysis of cascade structure with predictive control and feedback linearisation. *IEE Proceedings-Control Theory and Applications*, 152(3):317–324, 2005.

[12] Gene F Franklin, J David Powell, Abbas Emami-Naeini, and J David Powell. *Feedback control of dynamic systems*, volume 2. Addison-Wesley Reading, 1994.

[13] Manfred Morari and Jay H Lee. Model predictive control: past, present and future. *Computers & Chemical Engineering*, 23(4):667–682, 1999.

[14] Pavol Seman, Boris Rohal'-Ilkiv, Martin Juhás, and Michal Salaj. Swinging up the furuta pendulum and its stabilization via model predictive control. *Journal of Electrical Engineering*, 64(3):152–158, 2013.

[15] Anil V Rao. A survey of numerical methods for optimal control. *Advances in the Astronautical Sciences*, 135(1):497–528, 2009.

[16] John T Betts. Survey of numerical methods for trajectory optimization. *Journal of guidance, control, and dynamics*, 21(2):193–207, 1998.

[17] Wilson J Rugh and Jeff S Shamma. Research on gain scheduling. *Automatica*, 36(10):1401–1425, 2000.

[18] J. M. Lemos. Bayesian parameter estimation in nonlinear dynamic regression models. *Techical Report*, 26:10, 2009.

[19] Heinz Schättler and Urszula Ledzewicz. *Geometric optimal control: theory, methods and examples*, volume 38. Springer Science & Business Media, 2012.